J Mol Model (2013) 19:3875–3881
DOI 10.1007/s00894-013-1920-y

ORIGINAL PAPER

Theoretical study of photophysical properties of 1,4-dihydropyrrolo [3,2-b]pyrrole-cored branched molecules with thienylenevinylene arms toward broad absorption spectra for solar cells

Shanshan Tang · Binbin Tang · Dadong Liang · Guang Chen · Ruifa Jin

Received: 17 April 2013 / Accepted: 9 June 2013 / Published online: 3 July 2013

Abstract A series of oligo(thienylenevinylene) derivatives with 1,4-dihydropyrrolo[3,2-b]pyrrole as core has been investigated at the PBE0/6-31G(d) and the TD-PBE0/6-31+G(d,p) levels to design materials with high performances such as broad absorption spectra and higher balance transfer property. The results show that position and amount of arm affect the electronic density contours of frontier molecular orbitals significantly. The molecule with four arms owns the narrowest energy gap and the largest maximum absorption wavelength, and the molecule with two arms in positions *a* and *c* has the broadest absorption region among the designed molecules. Calculated reorganization energies of the designed molecules indicate that the molecules with two arms can be good potential ambipolar transport materials under proper operating conditions.

Keywords Charge transport property · Electronic and optical properties · Organic solar cells · Thienylenevinylene derivatives

Introduction

So far, a lot of effort has been devoted to the development of high-performance organic solar cell (OSC) materials [1–11]. For example, some studies indicate that branched oligothiophene and oligo(thienylenevinylene) derivatives can show excellent properties for OSC materials [12–14]. A theoretical study reported that 1,4-dihydropyrrolo[3,2-b]pyrrole-cored molecules were potential candidates for OSC materials [15, 16]. However, there still exist some challenges in the development of OSC materials. One of them is that, in present OSC devices, the photocurrent is limited because the overlap between the spectra of the sun and the absorption spectra of present organic materials for OSCs is not good [17]. The poor spectral overlap leads to the loss of the energy in the sunlight. The photons with energies below about 2.0 eV cannot be absorbed by the organic materials. Therefore, the spectral overlap is necessary to be increased, namely, the energy gap of π-conjugated molecule is necessary to be reduced. Understanding the relationship between molecular structure and charge transport property of material is a key factor for designing good candidates for OSC devices. The lower the reorganization energy, the higher the charge transfer rate [15, 16]. In this study, the charge transfer reaction is the

Electronic supplementary material The online version of this article (doi:10.1007/s00894-013-1920-y) contains supplementary material, which is available to authorized users.

S. Tang · D. Liang (✉)
College of Resource and Environmental Science,
Jilin Agricultural University, Changchun 130118, China
e-mail: dadongliang@126.com

B. Tang
School of Materials Science and Engineerning, Southwest Universsity, Chongqing 400715, China

G. Chen (✉)
College of Life Sciences, Jilin Agricultural University,
Changchun, Jilin 130118, China
e-mail: chg61@163.com

R. Jin
College of Chemistry and Chemical Engineering, Chifeng University, Chifeng 024000, China

self-exchange reaction. In other words, the free energy difference ($\Delta G°$) between the initial and final states is approximately assumed as zero in the transfer process. As a result, the charge transfer rate can be described by Marcus theory [18] via the following equation:

$$K = V^2/\hbar(\pi/\lambda k_b T)^{1/2}\exp(-\lambda/4k_b T) \quad (1)$$

where T is the temperature, k_b means the Boltzmann constant, λ represents the reorganization energy due to geometric relaxation accompanying charge transfer, and V is the electronic coupling matrix element (transfer integral) between the two adjacent species dictated largely by orbital overlap. It can be seen from Eq. (1) that there are two major parameters that determine the charge transfer rates: (i) V, which needs to be maximized, and (ii) λ, which needs to be small for significant transport. In order to investigate V, crystal data in general is required [19, 20]. However, the designed molecules may be non-crystal, and the electronic coupling matrix element value is very limited [21–24]. Though charge transfer integrals of amorphous dendrimers can be estimated [25–27], we cannot predict them for our designed molecules by similar methods due to the lack of available approaches. Thus, we focused on their reorganization energies to investigate their charge transport properties. Generally, the reorganization energy is determined by the fast change of the molecular geometry when a charge is added or removed from a molecule (the inner reorganization energy, λ_{int}) and represents variations in the surrounding medium due to the polarization effects (the external reorganization energy, λ_{ext}) [28–31]. Our designed molecules may be used as the donors of solar cells in solid films, because the dielectric constant of medium for molecule is low [21, 22]. The computed values of the external reorganization energy in pure organic condensed phases are not only small but also much smaller than their internal counterparts [32–34]. Moreover, previous works reported that there is a clear correlation between λ_{int} and charge transfer rate [25, 35, 36]. Therefore, we only paid attention to the discussion of the λ_{int} (reflects the geometric changes in the molecules when going from the neutral to the ionized state and vice versa) of the isolated active organic π-conjugated systems due to ignoring any environmental relaxation and changes in this paper. Hence, the electron reorganization energy (λ_e) and hole reorganization energy (λ_h) values can be calculated by Eqs. (2) and (3) [37]:

$$\lambda_e = \left[E_0^- - E_-\right] + \left[E_-^0 - E_0\right] \quad (2)$$

$$\lambda_h = \left[E_0^+ - E_+\right] + \left[E_+^0 - E_0\right]. \quad (3)$$

Where E_0^+ (E_0^-) is the energy of the cation (anion) calculated with the optimized structure of the neutral molecule. Similarly, E_+ (E_-) is the energy of the cation (anion) calculated with the optimized cationic (anionic) structure, E_+^0 (E_-^0) is the energy of the neutral molecule calculated at the cationic (anionic) state. Finally, E_0 is the energy of the neutral molecule at the ground state.

The ionization potential (*IP*) and electron affinity (*EA*) of the molecules were calculated as described in the formulas below:

$$IP = E(M^+) - E(M_{neutral}) \quad (4)$$

$$EA = E(M_{neutral}) - E(M^-) \quad (5)$$

where E ($M_{neutral}$) is the total energy of the neutral form at the optimized geometry, $E(M^+)$ and $E(M^-)$ are the total energies of the cationic and the anionic forms of the molecules, respectively.

In this contribution, we designed three groups of oligo(thienylenevinylene) derivatives with 1,4-dihydropyrrolo [3,2-b]pyrrole as the core and thienylenevinylene as the arms (see Scheme 1). The first group is the derivatives with two arms: **a-b**, **a-c**, and **a-d** are di-substitutions with thienylenevinylene arms in positions *a* and *b*, *a* and *c*, and *a* and *d*, respectively. The second group is the derivatives with three arms: **a-b-c** and **a-b-d** correspond to tri-substitutions with thienylenevinylene arms in positions *a*, *b*, and *c* and *a*, *b*, and *d*, respectively. The third group is molecules with four arms: **a-b-c-d** refers to tetra-substitutions of thienylenevinylene arms in positions *a*, *b*, *c*, and *d*. The highest occupied molecular orbital (HOMO) energies, the lowest unoccupied molecular orbital (LUMO) energies, the HOMO-LUMO gaps (E_g), and the absorption spectra were predicted. The electronic properties including natural bond orbital (NBO) charge, ionization potential (*IP*), electron affinity (*EA*), and reorganization energy (λ) were investigated. In addition, the correlation between these properties and the molecular structures was discussed.

Computational details

The quantum chemistry calculations of ground state were carried out with the aid of Gaussian 03 package [38]. The PBE0 method with the 6-31G(d) basis set was used in all the geometry optimization including neutral, cationic, and anionic molecules. A large number of previous works have suggested that the PBE0 method notably is adapted to the sulfur-bearing molecules [4–7, 15, 16, 39–44]. Frequency

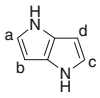

Core: 1,4-dihydropyrrolo[3,2-b]pyrrole

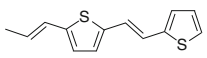

Arm: Thienylenevinylene

Scheme 1 Chemical structures of core and arm of investigated molecules. Core: 1,4-dihydropyrrolo[3,2-b]pyrrole Arm: Thienylenevinylene

calculations using the same methods as those for the geometry optimizations were performed for the investigated molecules. All real frequencies have confirmed the presence of a local minimum. The absorption spectra of the designed molecules were investigated by employing the TD-PBE0/6-31+G(d,p) method based on the optimized geometries obtained at the PBE0/6-31G(d) level. For comparing with the interested results reported previously [45, 46], the reorganization energies for electron (λ_e) and hole (λ_h) of the molecules were predicted from the single point energy at the B3LYP/6-31G(d,p) level. The natural bond orbital (NBO) analysis was used to map the charge distribution of the investigated molecules. Gaussian 09 package [47] was employed to optimize the geometry of molecules in excited state and calculate the NBO charge of ground and excited states.

Results and discussion

Frontier molecular orbitals

In order to gain insight into the influence of the optical and electronic properties, the electronic density contours of

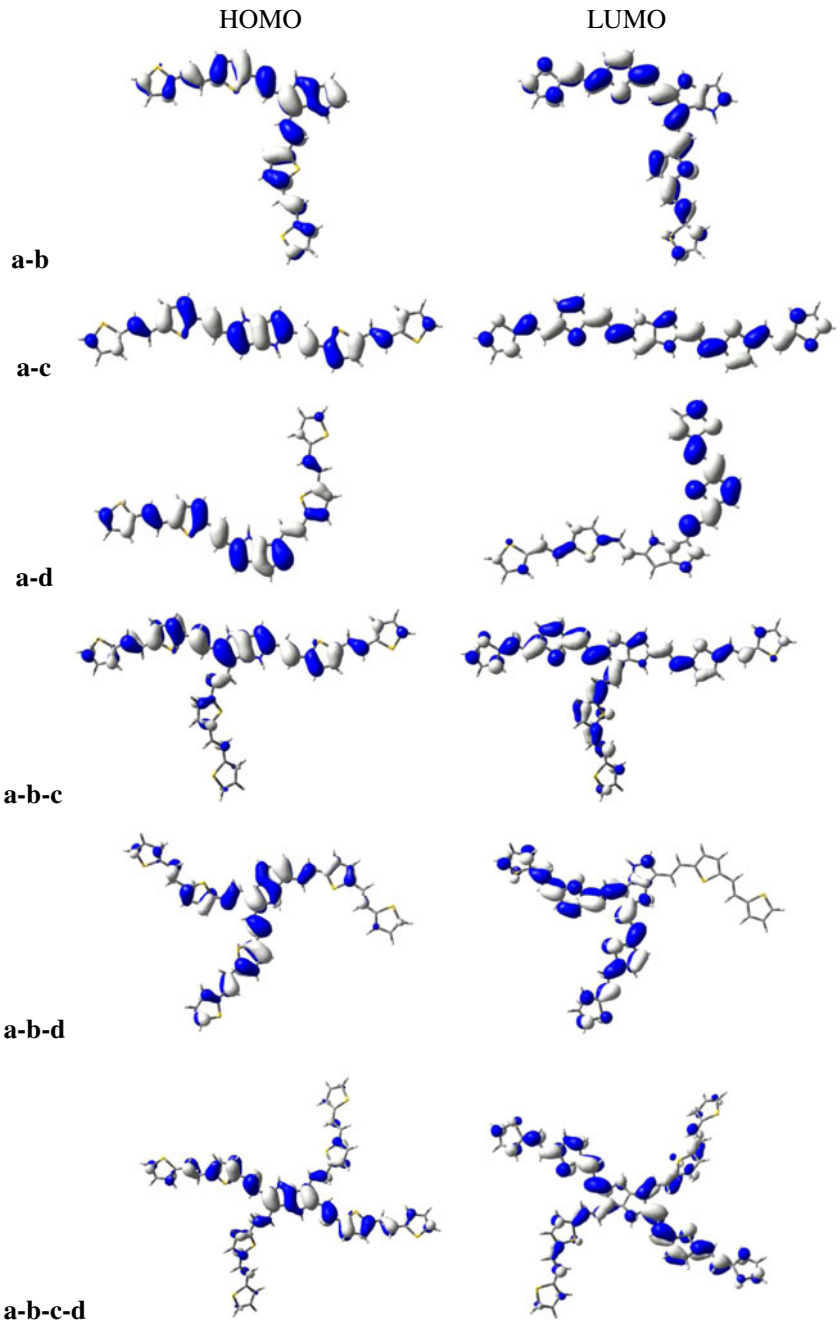

Fig. 1 Electronic density contours of the frontier molecular orbital for investigated molecules in ground state

frontier molecular orbitals (FMOs) for the designed molecules in ground and excited states are investigated, and their sketches are plotted in Fig. 1 and Fig. S1, respectively. The evaluations of FMO energies for designed molecules are shown in Fig. 2.

As shown in Fig. 1, for the molecules with two arms, the electronic density contours of FMOs of **a-b** and **a-c** are mainly delocalized on the whole molecules. The electronic density contours of HOMO of **a-d** is mainly spread over the core, one arm in position *a*, and half arm in position *d*. The electronic density contours of LUMO of **a-d** is mainly delocalized on one arm in position *d*, and with minor contributions of the core and the arm in position *a*. For the three arms molecules, the electronic density contours of FMO of **a-b-c** are mainly distributed on the core, two arms in positions *a* and *c*, and half arm in position *b*. The electronic density contours of HOMO of **a-b-d** is mainly centralized on the core, two arms in positions *a* and *b*, and half arm in position *d*. The electronic density contours of LUMO of **a-b-d** is mainly delocalized on the core and two arms in positions *a* and *b*. The electronic density contours of FMO of **a-b-c-d** are mainly spread over the core, two arm in positions *a* and *c*, and half arm in positions *b* and *d*. These results reveal that the position and amount of arm affect the distributions of the electronic density contours of FMO significantly. Except **a-d** displays a long-range electronic density reorganization during the excitation, the charge transfers of other molecules are rather localized, somehow being an undesired feature regarding the target electronic properties of the designed materials. That is to say, **a-d** will show better electron property.

The FMO energies are very important because they not only closely relate to the spectral properties but also to the reactivity of a compound. As shown in Fig. 2, for the two arms molecules, the HOMO energies (E_{HOMO}) are in the order of **a-c** > **a-b** > **a-d**, and their LUMO energies (E_{LUMO}) are in the order of **a-d** > **a-b** > **a-c**. Thus, their E_g values are in the order of **a-d** > **a-b** > **a-c**. These results display that for the two arms molecules, the arms in *a* and *c* positions result in the narrowest HOMO-LUMO gap. For the three arms molecules, the E_{HOMO}, E_{LUMO}, and E_g of **a-b-c** are higher, lower, and narrower than that of **a-b-d**, respectively. It indicates that the arm in position *c* leads to smaller E_g value than the arm in position *d*. The values of E_{HOMO}, E_{LUMO}, and E_g of **a-b-c** are larger, smaller, and smaller than that of **a-b**, respectively. It shows that increasing the arm in position *c* results in smaller E_g value. **a-b-c-d** owns the lowest E_{LUMO} and the narrowest E_g among the designed molecules. It should lead to the longest wavelength of absorption spectrum.

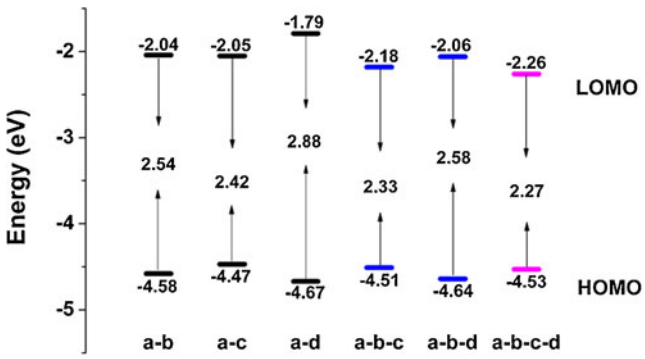

Fig. 2 Evaluation of the calculated FMOs energies for investigated molecules at the PBE0/6-31G(d) level

Absorption spectra

The values of longest wavelength of absorption spectrum (λ_{max}), corresponding oscillator strength (*f*), vertical excitation energy (E_v), and absorption region (*R* denotes for the difference of the longest and shortest wavelength values with oscillator strength larger than 0.01 considering the first twenty excited states, see Table S1, the Supporting information) of the designed molecules are listed in Table 1. The simulated absorption spectra of the investigated molecules are shown in Fig. 3.

For the molecules with two arms, the λ_{max}, corresponding *f*, and *R* values are all in the order of **a-c** > **a-b** > **a-d**, which is in good agreement with the corresponding reverse order of their E_v values. It reveals that the arms in positions *a* and *c* may result in large λ_{max} value and broad absorption region. For the three arms molecules, the λ_{max}, corresponding *f*, and *R* values are all in the order of **a-b-c** > **a-b-d**, and the E_v value of **a-b-c** is smaller than that of **a-b-d**. It shows that the arm in position *c* may lead to larger λ_{max}, *f*, and *R* values than the arm in position *d*, respectively. The λ_{max}, corresponding *f*, and *R* values of **a-b-c** are larger than that of **a-b**, which displays that increasing the arm in position *c* may increase the values of these properties. **a-b-c-d** has smaller E_v and larger λ_{max} values than that of **a-b-c**, which indicates that increasing the arm in position *d* can increase the λ_{max} value. In sum, the position and amount of the arm significantly influences optical properties of these designed molecules. As a

Table 1 Optical properties computed at the TD-PBE0/6-31+G(d,p)// PBE0/6-31G(d) level

	E_v (eV)	λ_{max} (nm)	*f*	*R* (nm)
a-b	2.15	577.77	1.61	298.51
a-c	2.07	599.40	3.33	314.80
a-d	2.43	510.20	1.27	232.59
a-b-c	1.98	627.15	2.11	312.61
a-b-d	2.12	584.21	0.91	272.09
a-b-c-d	1.94	640.68	2.05	286.89

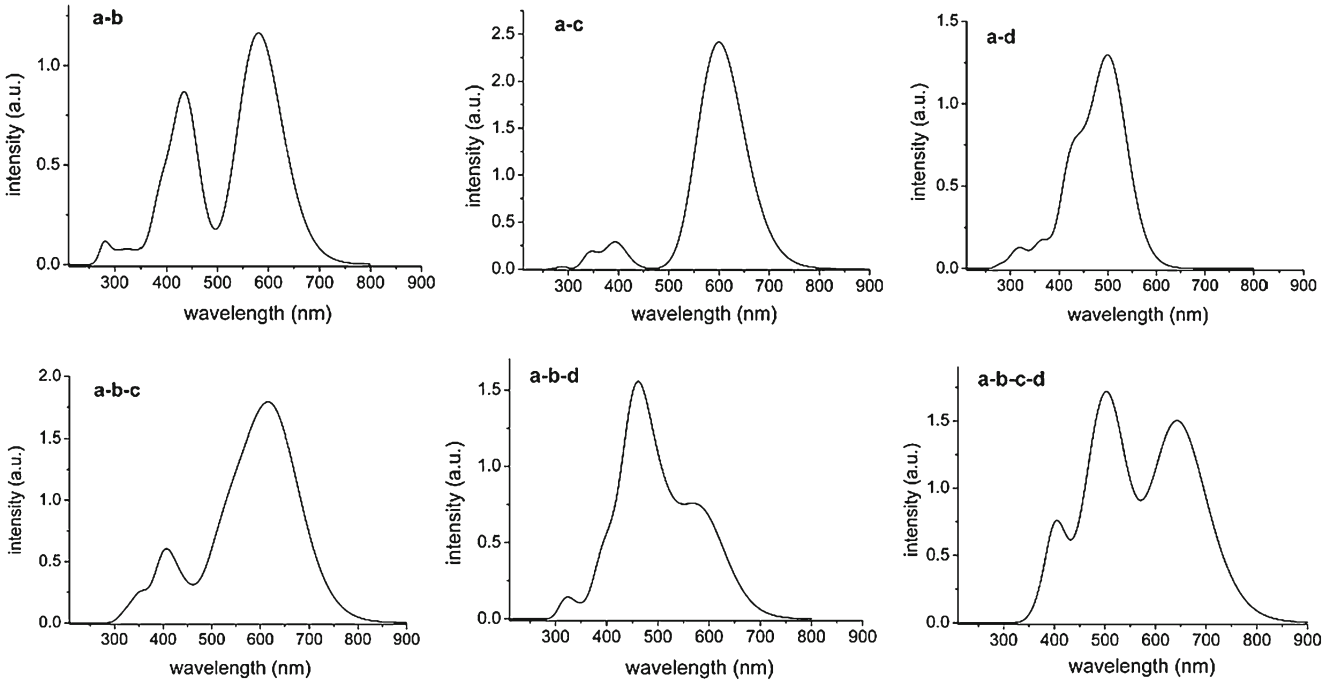

Fig. 3 Simulated absorption spectra of investigated molecules. The value of the full width at half maximum (fwhm) is 3000 cm^{-1}

result, **a-b** has the largest *f* and *R* values, and **a-b-c-d** has the largest λ_{max} value.

Charge transport properties

To compare the charge transport properties of the investigated molecules, we calculated the reorganization energies associated with different geometries of two states (anion and cation) based on the Eqs. (2) and (3). The results are summarized in Table 2. Herein, the reorganization energy is just the internal reorganization energy of the isolated active organic π-conjugated systems due to ignoring any environmental relaxation and changes. In order to study the response of the molecule to the formation of a hole, or to the addition of an electron, *IP* and *EA*, both vertical (v: at the geometry of the neutral molecule) and adiabatic (a: at the optimized structures of both the neutral and charged molecule) Eqs. (4) and (5) were computed. The calculated results are listed in Table 2. The natural bond orbital (NBO) analysis was supplied to map the charge distribution of the models and provide the evidence of charge transfer (see Fig. S2 and Tables S2-4, the Supporting information).

Table 2 Calculated molecular ionization potential (IP_a and IP_v), electron affinity (EA_a and EA_v), reorganization energies (λ_e and λ_h) computed at the B3LYP/6-31G(d,p)//PBE0/6-31G(d) level (in eV)

	IP_a	IP_v	EA_a	EA_v	λ_e	λ_h
a-b	5.230	5.335	1.308	1.124	0.269	0.223
a-c	5.103	5.202	1.365	1.202	0.224	0.214
a-d	5.350	5.427	1.034	0.913	0.143	0.186
a-b-c	5.043	5.128	1.606	1.419	0.259	0.197
a-b-d	5.194	5.265	1.419	1.251	0.245	0.171
a-b-c-d	4.990	5.066	1.740	1.570	0.223	0.169

It is well known the lower the *IP* of the hole-transport layer (HTL), the easier the entrance of holes from HTL to indium tin; the lower the *EA* of the electron-transport layer (ETL), the easier the entrance of electrons from ETL to cathode [37]. From the results in Table 2, one can see that the values of IP_a and IP_v are both in the order of **a-d** > **a-b** > **a-c**, and the values of EA_a and EA_v are both in the order of **a-d** < **a-b** < **a-c**. These results show that the orders of IP_a and IP_v values are nearly reversed with their orders of EA_a and EA_v values. On one hand, the IP_a and IP_v values of **a-b-c** are smaller than that of **a-b-d**. On the other hand, the EA_a and EA_v values of **a-b-c** are larger than that of **a-b-d**, respectively. The IP_a and IP_v values of **a-b-c** are smaller than that of **a-b**, respectively. It reveals that increasing the arm in position *c* can decease the IP_a and IP_v values. Among these molecules, **a-d** has the smallest EA_a and EA_v values, and **a-b-c-d** owns the smallest IP_a and IP_v values. It displays that **a-d** is the most proper one as ETL material, and **a-b-c-d** is the most proper one as HTL material.

For one thing, the λ_e values of designed molecules (0.143–0.269 eV) are smaller than that of tris(8-hydroxyquinolinato) aluminum(III) (Alq3) (λ_e=0.276 eV) which is a typical electron transport material [45]. It indicates that their electron transfer rates are higher than that of Alq3. On the other hand, their λ_h values (0.169–0.223 eV) are smaller than that of N,N′-diphenyl-N,N′-bis(3-methlphenyl)-(1,1′-biphenyl)-4,4′-

diamine (TPD) (λ_h=0.290 eV) which is a typical hole transport material [46]. It implies that their hole transfer rates are higher than that of TPD. Moreover, the differences between λ_e and λ_h values for **a-b**, **a-c**, and **a-d** are 0.046, 0.010, and 0.043 eV, respectively. It reveals that they have better equilibrium properties for hole- and electron-transport. As a result, these molecules are potential ambipolar charge transport materials under proper operating conditions. The values of λ_e and λ_h are both in the order of **a-b** > **a-c** > **a-d**, which shows that the arms in positions *a* and *d* may lead to better charge transfer rate. The values of λ_e and λ_h of **a-b-c** are larger than that of **a-b-d**, respectively. Among these designed molecules, **a-d** has the smallest λ_e value, and **a-b-c-d** owns the smallest λ_h value. These designed molecules are potential candidates as hole transfer materials toward solar cells expect **a-d**, because their λ_h values are smaller than their λ_e values, respectively.

From Figs. 1 and S1 (Supporting information), one can find that the electronic density contours of FMOs for molecules in excited state are similar in ground state, respectively. These results show that the donor and accepter are the whole molecules for **a-b** and **a-c**. The donor of **a-d** is the core, one arm in position *a*, and half arm in position *d*, and its acceptor is the arm in position *d*. The donor and acceptor of **a-b-c** are the core, two arms in positions *a* and *c*, and half arm in position *b*. The donor of **a-b-d** is the core, two arms in positions *a* and *b*, and half arm in position *d*, and its acceptor is the core and two arms in positions *a* and *b*. The donor and acceptor of **a-b-c-d** are the core, two arms in positions *a* and *c*, and half arm in positions *b* and *d*. Figure S2 and Tables S2-4 (Supporting information) suggest that there is charge transfer during the excitation. It agrees with the results obtained in electronic density contours of FMOs for molecules.

Conclusions

In the present work, we report a theoretical investigation of predicting the effects of position and amount of arm on optical and electronic properties for a series of 1,4-dihydropyrrolo[3,2-b]pyrrole-cored branched molecules with thienylenevinylene arms. The following conclusions can be drawn. (1) The position and amount of arm affect the distributions of the FMO patterns significantly. (2) **a-b-c-d** owns the lowest E_{LUMO} and the narrowest E_g, and increasing the arm in position *c* results in smaller E_g value. (3) **a-b** has the largest *f* and *R* values, and **a-b-c-d** has the largest λ_{max} value. (4) **a-d** is the most proper one as ETL material, and **a-b-c-d** is the most proper one as HTL material. (5) **a-d** has the smallest λ_e value, and **a-b-c-d** owns the smallest λ_h value. These results can be helpful for further theoretical and experimental study of oligo(thienylenevinylene) derivatives toward the application as OSC materials.

Acknowledgments Financial support from the Science Foundation for Young Teachers of Jilin Agricultural University (No. 201219) is gratefully acknowledged.

References

1. Kim JY, Lee K, Coates NE, Moses D, Nguyen TQ, Dante M, Heeger AJ (2007) Science 317:222–225
2. Sang-aroon W, Laopha S, Chaiamornnugool P, Tontapha S, Saekow S, Amornkitbamrung V (2013) J Mol Model 19:1407–1415
3. Zhang WB, Tu YF, Sun HJ, Yue K, Gong X, Cheng Stephen ZD (2012) Sci China Chem 55:749–7540
4. Tang SS, Zhang JP (2011) Inter J Quantum Chem 111:2089–2098
5. Tang SS, Zhang JP (2011) J Phys Chem A 115:5184–5191
6. Liang DD, Liu JB, Kang LJ, Jin RF, Tang SS (2012) Mol Phys 110:369–375
7. Liang DD, Tang SS, Liu JB, Liu JH, Kang LJ (2009) J Mol Struct THEOCHEM 908:102–106
8. Cheng YJ, Yang SH, Hsu CS (2009) Chem Rev 109:5868–5923
9. Gutiérrez-Pérez RM, Flores-Holguín N, Glossmann-Mitnik D, Rodriguez-Valdez LM (2011) J Mol Model 17:1963–1972
10. López AM, Mateo-Alonsobc A, Prato M (2011) J Mater Chem 21:1305–1318
11. Zhang CR, Liu L, Zhe JW, Jin NZ, Yuan LH, Chen YH, Wei ZQ, Wu Y-Z, Liu ZJ, Chen HS (2013) J Mol Model 19:1553–1563
12. Fichou D (ed) (1999) Handbook of oligo- and polythiophenes. Wiley-VCH, Weinheim
13. Vélez JH, Gutiérrez-Oliva S, Díaz FR, Angelica del Valle M, Toro-Labbé A, Bernède JC, East GA (2011) J Mol Model 17:81–88
14. Müllen K, Wegner G (eds) (1998) Electronic materials: The oligomer approach. Press: Wiley-VCH, Weinheim
15. Tang SS, Zhang JP (2012) J Comput Chem 33:1353–1363
16. Hu B, Yao C, Wang QW, Zhang H, Yu JK (2012) Sci China Chem 55:1364–1369
17. Winder C, Sariciftci NS (2004) J Mater Chem 14:1077–1086
18. Marcus RA (1993) Rev Mod Phys 65:599–610
19. Marcus RA (1964) Theo Annu Rev Phys Chem 15:155–196
20. Hush NS (1958) J Chem Phys 28:962
21. Yang XD, Wang LJ, Wang CL, Long W, Shuai ZG (2008) Chem Mater 20:3205–3211
22. Wang CL, Wang FH, Yang XD, Li QK, Shuai ZG (2008) Org Electron 9:635–640
23. Troisi A, Orlandi G (2006) J Phys Chem A 110:4065–4070
24. Yin SW, Yi YP, Li QX, Yu G, Liu YQ, Shuai ZG (2006) J Phys Chem A 110:7138–7143
25. Köse ME, Mitchell WJ, Kopidakis N, Chang CH, Shaheen SE, Kim K, Rumbles G (2007) J Am Chem Soc 129:14257–14270
26. Nelsen SF, Trieber DA, Ismagilov RF, Teki Y (2001) J Am Chem Soc 123:5684–5694
27. Nelsen SF, Blomgren F (2001) J Org Chem 66:6551–6559
28. Käse ME, Long H, Kim K, Graf P, Ginley D (2010) J Phys Chem A 114:4388–4393
29. Köse ME, Graf P, Kopidakis N, Shaheen SE, Kim K, Rumbles G (2009) Chemphyschem 10:3285–3294
30. Lemaur V, Steel M, Beljonne D, Brédas JL, Cornil J (2005) J Am Chem Soc 127:6077–6086
31. Cheung DL, Troisi A (2010) J Phys Chem C 114:20479–20488
32. Norton JE, Brédas JL (2008) J Am Chem Soc 130:12377–12384
33. Martinelli NG, Idé J, Sánchez-Carrera RS, Coropceanu V, Brédas JL, Ducasse L, Castet F, Cornil J, Beljonne D (2010) J Phys Chem C 114:20678–20685
34. Mc Mahon DP, Troisi A (2010) J Phys Chem Lett 1:941–946

35. Sakanoue K, Motoda M, Sugimoto M, Sakaki S (1999) J Phys Chem A 103:5551–5556
36. Hutchison GR, Ratner MA, Marks TJ (2005) J Am Chem Soc 127:2339–2350
37. Zou LY, Ren AM, Feng JK, Liu YL, Ran XQ, Sun CC (2008) J Phys Chem A 112:12172–12178
38. Frisch MJ et al. (2003) Gaussian 03, Revision B.03. Gaussian, Inc, Pittsburgh
39. Gahungu G, Zhang B, Zhang JP (2007) J Phys Chem C 111:4838–4846
40. Hu B, Yao C, Huang XR (2012) Spectrosc Lett 45:17–21
41. Jacquemin D, Perpete EA (2006) Chem Phys Lett 429:147–152
42. Perpete EA, Preat J, Andre JM, Jacquemin D (2006) J Phys Chem A 110:5629–5635
43. Jacquemin D, Wathelet V, Perpete EA (2006) J Phys Chem A 110:9145–9152
44. Jacquemin D, Preat J, Wathelet V, Fontaine M, Perpete EA (2006) J Am Chem Soc 128:2072–2083
45. Lin BC, Cheng CP, You ZQ, Hsu CP (2005) J Am Chem Soc 127:66–67
46. Gruhn NE, da Silva Filho DA, Bill TG, Malagoli M, Coropceanu V, Kahn A, Brédas JL (2002) J Am Chem Soc 124:7918–7919
47. Frisch MJ et al. (2009) Gaussian 09. Gaussian, Wallingford